ECS Transactions, 3 (7) 539-549 (2006)
10.1149/1.2355851, copyright The Electrochemical Society

Characterization and Modeling of Atomically Sharp "Perfect" Si:Ge/SiO_2 Interfaces

W. Windl[a], T. Liang[a,b], S. Lopatin[c], and G. Duscher[c,d]

[a] Department of Materials Science and Engineering, The Ohio State University, Columbus, Ohio 43210, USA
[b] Department of Materials Science and Engineering, Florida State University, Gainesville, Florida 32611, USA
[c] Department of Materials Science and Engineering, North Carolina State University, Raleigh, North Carolina 27606, USA
[d] Solid State Division, Oak Ridge National Laboratory, Oak Ridge, Tennessee 37831, USA

Using ab-initio calculations and atomic-resolution Z-contrast imaging and electron energy-loss spectroscopy, we show that oxidation of a germanium-implanted Si surface can produce an atomically-sharp interface with a band structure that seems to be more favorable for use in electronic devices than the usually diffuse interface in Si/SiO_2. Furthermore, we propose an ab-initio based Monte-Carlo model to simulate oxidation of SiGe alloys to better understand the formation of the sharp interface.

Introduction

Thermally grown SiO_2 is an excellent dielectric, an effective barrier to dopant diffusion, and can be selectively etched, which enables the fabrication of integrated circuits. State-of-the-art device technology requires the reduction of the gate-oxide film thickness to as thin as ~1.2 nm. Previous studies have shown that the interface between Si and thermally grown SiO_2 is not chemically abrupt, but has a transition region of "suboxide" with intermediate Si oxidation states Si^{1+}, Si^{2+} and Si^{3+}, where the Si atoms have neither zero (Si^{0+}, *i.e.*, bulk Si) nor four (Si^{4+}, *i.e.*, bulk SiO_2) oxygen neighbors (8, 10).

A recent extension of the traditional silicon technology is the mixing of germanium into the silicon wafer material to enhance performance (1). One of the interesting advances in this area has been achieved by Fathy, Holland, and White who demonstrated the formation of SiO_2 on nearly pure epitaxial layers of Ge on Si substrates with a flat interface (2). This flat interface was achieved by Ge implantation and wet oxidation at sufficiently high oxidation temperatures (> 700 ^oC) and high Ge doses (~10^{16} cm^{-2}). However, SiGe/SiO_2 systems have been found to have significantly worse electrical properties than Si/ SiO_2 systems (3, 4). Among the discussed possible causes for this were the nature of the interface, specifically the detrimental role of larger quantities of the intermediate Si oxidation states, and the presence of elemental Ge at the interface (3).

These poor electrical properties have kept the industry for a long time from using SiGe as a device material. In the following, we try to demonstrate that devices fabricated by Fathy *et al.*'s "snow plowing" process seem to have a very abrupt, nearly "perfect" interface between the substrate and the oxide, and that Ge in the oxide seems to be the probable culprit for decreased device properties. Since abruptness greatly affects the performance of small devices (5), the atomically sharp Ge/SiO_2 interface is quite remarkable, especially since such an abruptness (at least to date) has never been observed in conventional Si/SiO_2 structures (6).

Experiment: *Z*-Contrast and Electron Energy Loss Spectroscopy

Z-contrast spectroscopy images the projection of the atomic columns of a crystalline sample oriented to a low-order zone axis by scanning it with the focused electron probe of a scanning transmission electron microscope (STEM) (7). Since high-angle scattering depends on the atomic number (squared), the acquired *Z*-contrast image also contains information about the sample composition. Electrons scattered to low-angles can be used for simultaneous EELS, where core electrons are excited into the conduction band. The resulting core-loss edges are closely related to the conduction-band density of states (DOS) (8). Since the DOS depends on the atomic species and the bonding to the neighboring atoms, EELS provides complimentary information about the examined structure.

In the examined sample, the pile-up lead to a compact Ge layer which contained, within our experimental detection limit of about 5 atomic percent, no Si atoms as probed by EELS. Figure 1(a) shows a typical Z-contrast image of our sample with the substrate side aligned along the [110] direction. The Ge layer is brighter since Ge is heavier then Si. The ellipse-like bright double spots correspond to atomic columns. The distance between those columns in (110) projection is 0.14 nm in Ge (larger than the electron probe size) and can be resolved. The dumbbell structure is clearly seen as double peaks in the intensity profile across the Si/Ge/SiO_2 interface in Fig. 1(b). We did not find any atomic layer steps at the crystalline side of the interface in any of the studied samples, which suggests an atomically flat interface.

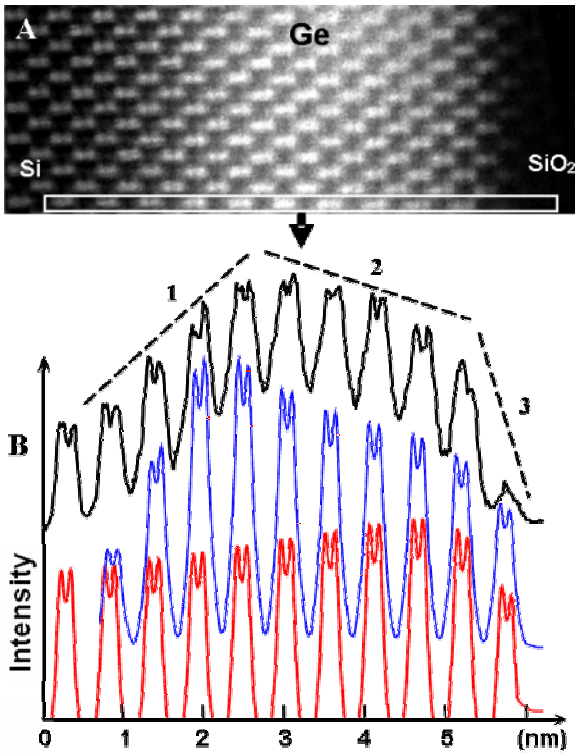

Figure 1. (a) Z-contrast image of Si substrate with Ge film covered by SiO_2; (b) signal intensity profile across the interface from experiment (upper line) and from simulation using the concentration profiles from Fig. 5(c) (lowest line) and 5(d) (middle line), respectively.

Different slopes can be identified in the experimental intensity profile [Fig. 1(b)]. Slope 1 results from the atomic mass increase at the transition from Si to Ge, which extends over 3-4 dumbbell layers (about 1 nm). Slope 2 shows a nearly linear decrease in Ge concentration, which will be discussed in Sec. IV. The sudden drop in intensity (slope 3) indicates a compositional change in the last dumbbell layer before the interface. Thus, nearly all of the compositional change from pure Ge to SiO_2 takes place within approximately one transitional layer right below the interface.

To gain insight into the atomic configuration of the Ge/SiO_2 interface and Si oxidation states we also employed EELS measurements of the Si-$L_{2,3}$ edge in comparison to theoretical spectra. The latter were calculated as described by Duscher *et al*. (8), who have shown that the Z+1 approximation, where the examined atom is replaced by the element with atomic number Z+1 in order to compensate for the core-hole shift that is caused by the electron-excitation process, predicts the near-edge EELS spectrum reasonably well within standard pseudopotential density-functional calculations.

At Si/SiO_2 interfaces, one finds the Si-$L_{2,3}$ edge onset in the crystalline Si part (Si^{0+}) to be at 99.8 eV with a first maximum at about 101 eV (Fig. 2, Si^{0+} spectrum; Fig. 3(a), spectrum 5), whereas the SiO_2 spectrum (Si^{4+}) is characterized by main absorption features at 106 and 108 eV (Fig. 2, Si^{4+} spectra; Fig. 3(a), spectrum 1) (9). The intermediate oxidation states (Si^{1+}, Si^{2+}, Si^{3+}, shown in Fig. 2) have absorption features between those of Si^{0+} and Si^{4+}, as shown by photoemission spectroscopy (10) and theoretical calculations (11). EELS measurements at the graded interface between Si and SiO_2 contain a mix of the different oxidation states, resulting in a nearly linear spectrum onset (Fig. 3(a), spectra 2 and 3). Stoichiometric SiO_2 appears no sooner than 0.5 nm away from the interface. Thus, the interface extends over approximately three layers – depending on how one defines a layer – and is not chemically abrupt.

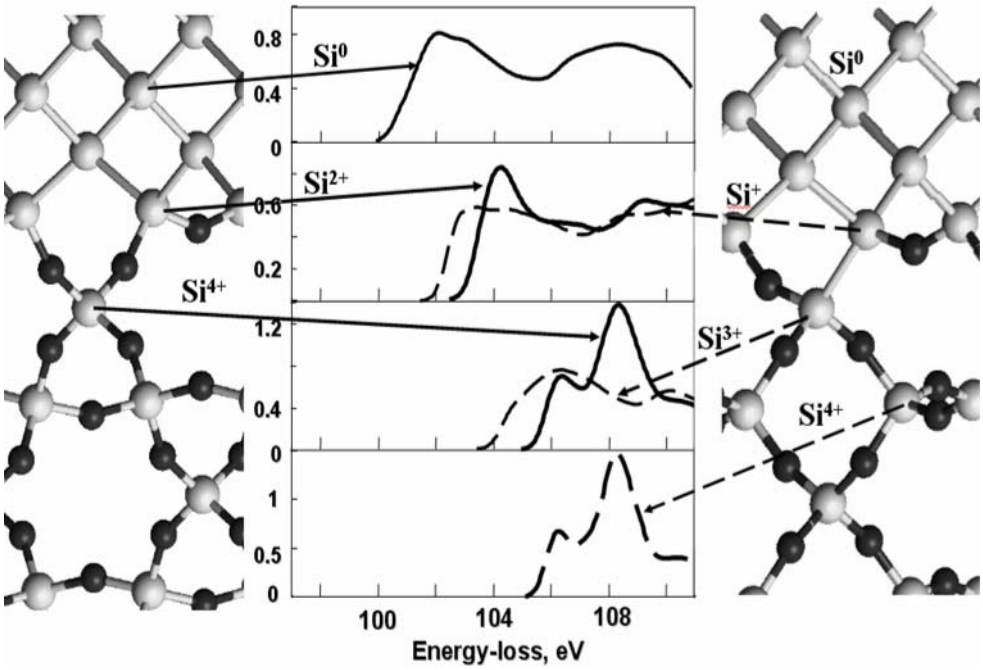

Figure 2. Theoretical Si-$L_{2,3}$ edge at the Si/SiO_2 interface, calculated by a combination of all-electron calculations for the onset energy and density-functional pseudopotential calculations within the Z+1 approximation (8).

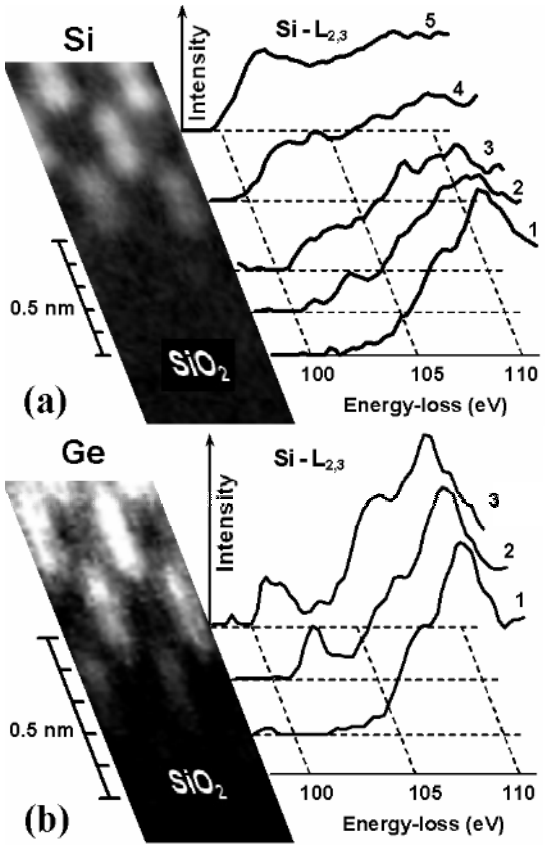

Figure 3. Line-scan EELS of the Si-$L_{2,3}$ ionization edge across the (a) Si/SiO_2 interface and (b) Ge/SiO_2 interface.

This is in stark contrast to our measured EELS spectra for the Ge/SiO_2 sample, which are shown in Fig. 3(b). All spectra show strong Si^{4+} signals from the surface oxide, since this sample is extremely thin. This Si^{4+} signal might be further increased by the delocalization of the inelastic scattering process. This poses no problem, since the following analysis is based on the signals of the oxidation states less than 4+.

Only 2 Å away from the last crystalline layer on the amorphous side we observe no ionization edge other than completely oxidized Si^{4+} (Figure 3(b), spectrum 1 Fig. 2, Si^{4+} spectrum). One layer away from the oxide at the first crystalline layer, a clear signal of Si^{2+} appears (Fig. 3(b), spectrum 2; compare to Fig. 2, Si^{2+} spectrum) (10, 11). In the second crystalline layer, we find the signal of bulk Si (Si^{0+}) with the modifications typical of bulk SiGe (Fig. 2(b), spectrum 3), which looks different from pure Si due to the core level shift caused by Ge (12). The EELS data analysis from subsequent atomic layers on the crystalline side of the interface shows that within one or two atomic layers the Si concentration falls below the detection limit, which we estimate to be less than 5 atomic percent. No linear intensity increase typical of the mix of suboxide oxidation states in non-abrupt Si/SiO_2 interfaces is detected. Thus, our data suggest an atomically sharp interface for this structure, with one transition layer, containing only Si^{2+}, after the last crystalline layer and pure oxide after only ~2 Å, which had been never observed before in electronic devices. These findings are consistent with recent high-temperature oxidation results (13) in which, however, no atomically abrupt interface has been observed. Our findings are in contrast with previous work (3, 14) but those studies dealt with higher Ge concentrations or lower oxidation temperatures.

Band Structure Calculations

The advantage of a chemically abrupt interface between a semiconductor and a dielectric becomes apparent when the required thickness for the gate dielectric reaches the scale of 1 nm. We demonstrate this with the help of density functional calculations of the real-space projected DOS for different structures of interfaces between Si (or Ge/Si) and thin SiO_2 layers.

First we calculated the DOS for the non-abrupt Si/SiO_2 interface (Fig. 4(a)) containing a transitional region with a mixture of suboxide states $Si^{1+/2+/3+}$ (a model adopted from Ref. (27)). This interface displays a gradual opening of the oxide band gap over about 0.5 nm (Fig. 4(b)) in excellent agreement with our experimental EELS data (Fig. 4(c)). The gradual opening of the suboxide band gap causes a considerably higher charge-carrier density than in stoichiometric oxide, since the electron concentration in the conduction band depends exponentially on the energy difference between the conduction band edge

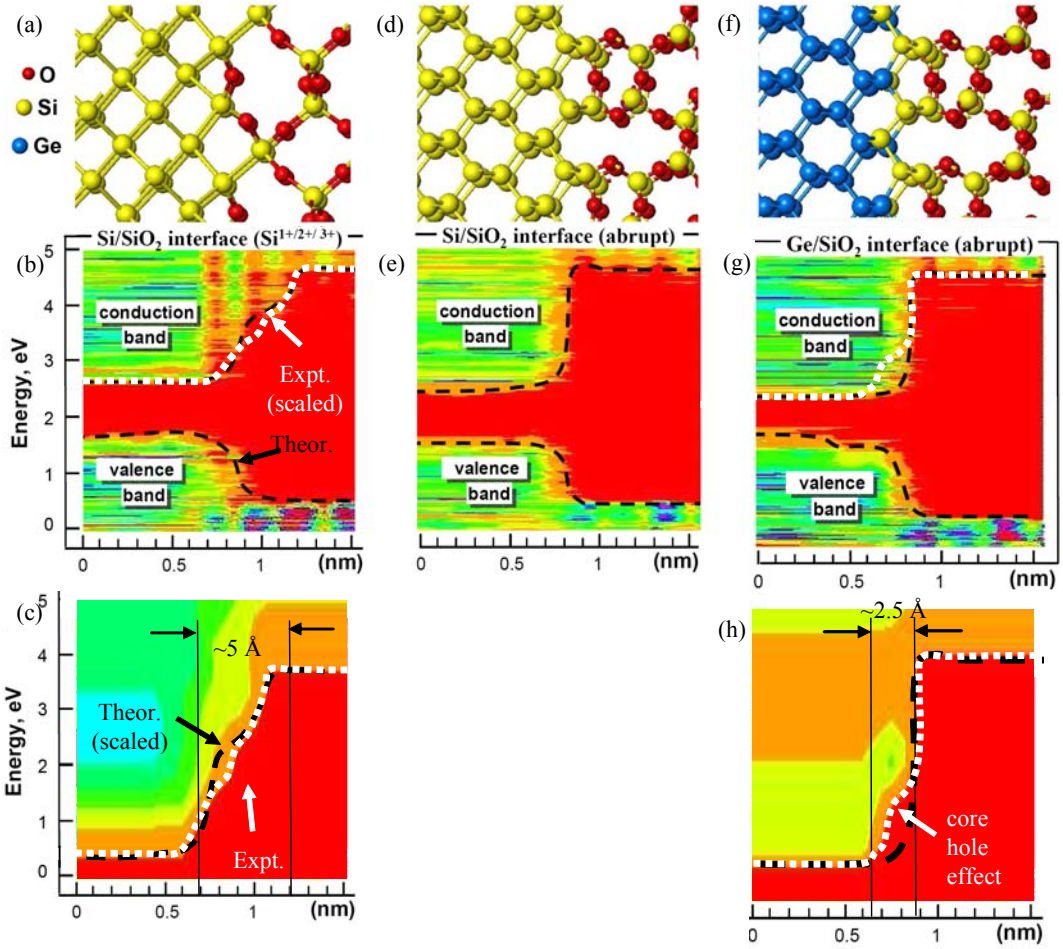

Figure 4. Calculated and measured band line-ups around interface. Model interface structures and corresponding DOS simulations in comparison to experimental EELS: (a)-(c), non-abrupt Si/SiO_2 interface with suboxide region containing $Si^{1+}/Si^{2+}/Si^{3+}$ oxidation states; (d) and (e), the abrupt Si/SiO_2 interface; (f)-(h), the abrupt Ge/SiO_2 interface. Results for DOS are shown in temperature scale - higher temperature (red) corresponds to a lower density of available electron states. All structures are H-terminated slabs with periodic boundaries parallel to the interface, resulting in confinement-enhanced band gaps as compared to periodic DFT calculations.

E_c and the Fermi energy E_F, $n = n_0 \exp[-(E_c - E_F)/(k_B T)]$ (analogous for holes). The resulting decreased charge separation between channel and gate thus increases the minimum possible thickness of a functional gate oxide.

The hypothetical abrupt Si/SiO_2 interface with only one transitional layer of Si^{2+} would not interpose such a problem. As shown in Fig. 4(d) and (e), this interface would have a highly desirable band line-up with a sharp transition from Si to SiO_2.

Our simulations suggest that the band structure (and thus, the electrical properties) of the abrupt Ge/SiO_2 interface (Fig. 4(f) and (g)) are comparable to the case of the hypothetical abrupt Si/SiO_2 interface in Fig. 4(c) and (d), in excellent agreement with our EELS data (Fig. 4(h)), apart from the core-hole intensity on the Si side of the EELS data[3]. Thus, it is surprising to find our experimental results consistent with the model of atomically abrupt Ge/SiO_2 interface. Those results have an additional technological relevance, since we can show that such abrupt Ge/SiO_2 interfaces have a band structure superior to those of the to-date known gradual Si/SiO_2 interfaces.

Ab-Initio Based Monte Carlo Modeling of SiGe Oxidation

Oxidation Model

A reaction-diffusion model (15) for the oxidation of silicon-germanium alloys and a kinetic lattice Monte Carlo model (16) for the formation of Ge nanocrystals in Ge^+ implanted SiO_2 layers have been suggested in the past, both based on phenomenological reaction and diffusion parameters. However, we could not find previous Monte-Carlo work for the oxidation process.

We have recently suggested such a model (17) based on atomistic, mass-transport limited oxidation. There, oxygen atoms are added in random, not-yet oxidized bonds between neighboring Si atoms. The selection of the random oxidation site is biased by the solution of Fick's 2nd equation for in-diffusion with constant surface concentration, which is a complimentary error function. This makes it most probable that Si-Si bonds closest to the surface are oxidized.

Simultaneously with the addition of oxygen atoms, we randomly switch Ge and Si neighbors to simulate the diffusion that takes place at elevated oxidation temperatures. These switches are accepted or rejected with the usual Metropolis algorithm (18) depending on the change in the total energy, which is approximated by an analytical function of the number of Si-Si, Si-Ge, Ge-Ge, Si-O-Si, Si-O-Ge, and Ge-O-Ge bonds fitted to ab-initio calculations (17),

$$E[\mathrm{eV}] = -2.71 n_{\mathrm{SiSi}} - 2.23 n_{\mathrm{GeGe}} - 2.47 n_{\mathrm{SiGe}} - 7.07 n_{\mathrm{GeOGe}} - 8.94 n_{\mathrm{SiOSi}} - 8.05 n_{\mathrm{SiOGe}}. \qquad [1]$$

This expression indicates that the formation of Ge-O-Ge and Si-O-Ge bonds will dramatically increase the system energy as compared to Si-O-Si bonds. In other words, from an energetics point of view, Ge atoms "prefer" to stay away from the oxide region.

For a sensible simulation of the snowplowing effect, a realistic ratio between oxidation rate and diffusivity is a key ingredient. For the former, we choose a rate commensurate with experimental oxidation rates and theoretical results for O_2 and H_2O diffusion through SiO_2 (4, 16, 19).

For the latter, we assume – due to lack of better knowledge – intrinsic diffusion. Since Ge is the much more mobile atom in the alloy, only hopping of Ge is considered. On the Si side of the interface, the local-concentration dependent hopping rates were ad-

justed to experimental results of intrinsic Ge diffusion in SiGe alloys (20), which we fit with a quadratic concentration dependence of prefactor and activation energy (Fig. 5) (17),

$$D(x,T) = D_0(x)\exp\left(-\frac{E_0(x)}{k_B T}\right),$$
$$D_0(x) = \exp\left(7.01 - 22.16x + 18.67x^2\right), \qquad [2]$$
$$E_0(x) = \quad 4.66 - \ 5.25x + \ 3.70x^2.$$

We are aware of recent work that suggests that the activation energy is non-continuous with concentration (21), but neglect this for now. For the concentration dependence, we calculate the fraction of Ge atoms in each atomic layer of the Si part of our simulation cell. Since Ge diffusion in SiO_2 is significantly slower than in Si (22), we assume that Ge atoms are immobile once they are surrounded by oxide (17). In the interface region, we keep the Ge on the oxide side mobile using the same Ge-concentration dependent diffusion coefficient as on the Si side for the first three oxide layers, which our EELS measurements have found to be transition layers (see second section).

Since, as we will see in the following, the diffusivity around the interface is the most critical parameter and cannot be determined conclusively from experiment, we are currently working on the ab-initio calculation of the Ge diffusivity in SiO_2 and at the interface with a methodology we had used previously for B in Si (23). However, we found strong interactions of Ge with O vacancies and H atoms, which increase the phase space considerably and make the calculation tedious in addition to the already existing complexity from the competing diffusion mechanisms (21).

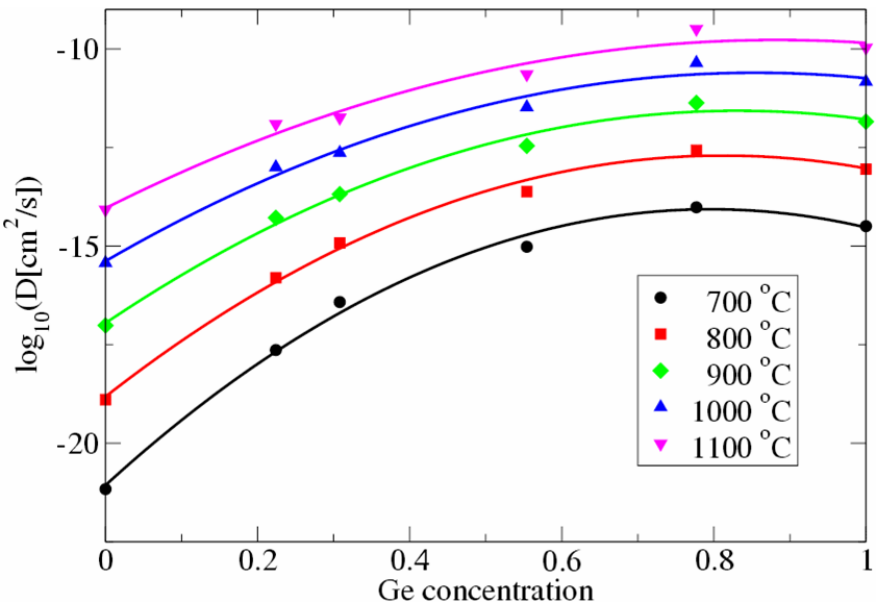

Figure 5. Experimental diffusivities of Ge in Si as a function of Ge concentration and temperature (points) (20). Arrhenius fit (lines) with activation energy and prefactor as quadratic functions of the Ge concentration, *x*, as given in Eq. (4).

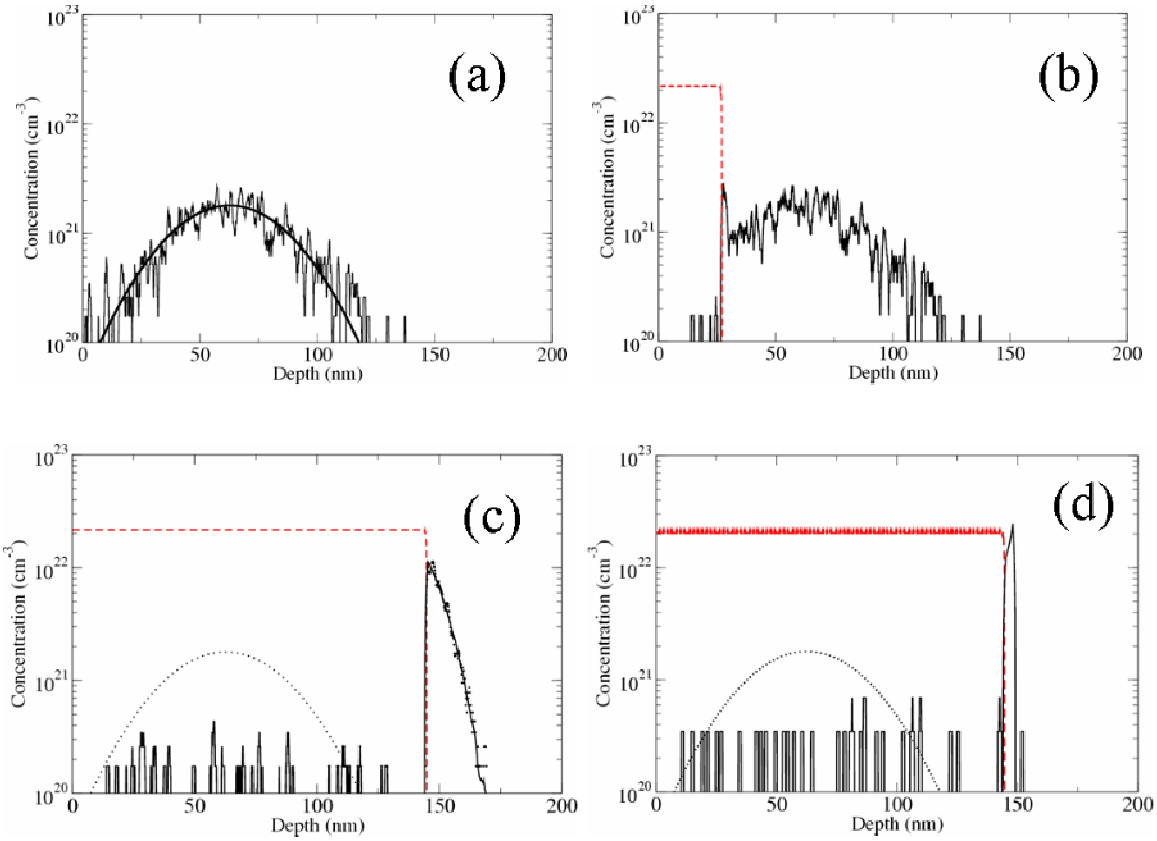

Figure 6. (a) Starting distribution of Ge vs. depth before oxidation (thick line is dual-Pearson fit). Simulated O (dashed line) and Ge (solid line) concentration profiles for oxidation at 1000 ^{o}C after (b) 9 min and (c) 48 min (initial dual-Pearson profile shown by dotted line; in main-peak area (~150 nm), instantaneous profile shown by dots, average over 200 profiles shown as solid line). (d) Simulation result for limited Ge diffusivity in Si, resctricted to ~30 atomic layers below the oxidation front.

Results & Discussion

In this section, we apply the previously discussed oxidation/diffusion model to the experimental structure by Fathy *et al.* discussed before (2). To start from the same initial distribution, we first simulate the implanted profile for a dose of 10^{16} cm^{-2} Ge, implanted with an energy of 100 keV into Si, using the efficient and highly predictive REED-MD program (24). The resulting concentration-vs.-depth profile has been translated into a random distribution of Ge atoms in a 1.1×8.7×199.8 nm^3 simulation cell as shown in Fig. 6(a). Kinetic simulations for such a cell, which in principle contains more than 94,000 Si atoms and adds per oxidized Si layer 64 O atoms, becomes easily feasible within the Monte Carlo approach, where only O and Ge atoms are tracked, whereas the Si atoms only define the lattice sites.

The mechanism of the snow-plowing effect that leads to the Ge pile-up can be well demonstrated within this model. Our Monte Carlo simulation results for temperature and Ge dose equal to the processing of the sample discussed in Sec. II are shown in Fig. 6. At this temperature, Ge becomes mobile in the Si matrix within our model, and is also ejected out of the growing oxide at an appreciable rate due to the strong repulsive interaction between Ge and O (Eq. [1]). This results in the formation of pure SiO_2 right above an

increasing pile-up of Ge as shown in Fig. 6(b)-(d). However, once the Ge concentration reaches about 2×10^{21} cm^{-3} [Fig. 6(b)], the oxide starts to incorporate Ge. During subsequent oxidation, the pile-up saturates at a maximum Ge concentration of 1×10^{22} cm^{-3} (~20 at.%), with an exponential drop of the concentration below the oxidation front [Fig. 6(c)]. The drop-off width of the Ge profile is approximately 15 nm per decade. Further oxidation just pushes this profile more or less unchanged deeper into the substrate. From the concentration profile, one can easily determine a Z-contrast intensity profile by multiplying Airy functions for each layer with the corresponding Ge and Si concentrations times Z^2 [Fig. 1(b)].

Thus, our predicted profile is different from the experimental findings [Fig. 1(b)], where the Ge pile-up had been found to reach a concentration of supposedly close to 100 at.% in a compact layer of about 4-5 nm thickness. The most probable explanation for the discrepancy would involve the Ge diffusivity in Si. From experiment, it is found that at the simulated temperature of 1000 ^{o}C, Ge diffusion takes place to 60-70% via the vacancy mechanism (25). On the other hand, oxidation has been found to inject a supersaturation of interstitials (and a corresponding decrease in vacancy concentration) into the substrate and thus to accelerate interstitial diffusers while retarding atoms diffusing via the vacancy mechanism (26). From that, we expect the Ge diffusivity to be significantly lower than the equilibrium diffusivity that we use. One possibility is shown in Fig. 6(d), where the simulation assumes that the Ge diffusivity is only equal to the intrinsic value close to the interface and decays to zero over the next 30 atomic layers (assuming that by that distance the interstitial supersaturation should completely control the point defect concentrations and prevents vacancy-assisted Ge diffusion).With such a model, we indeed can reproduce the experimental findings, especially slope 2 in the Z-contrast profile in Fig. 1(b). Before a final answer can be given, further work, especially examining the point-defect equilibrium close to the interface, is needed and presently on-going (including the significant fact that the implanted Ge dose should amorphize the Si substrate, which is neglected in our discussion).

Independent of this, our model predicts that what was originally interpreted as pure SiO_2 might indeed contain a small amount of Ge. With a subsequent TEM measurement at a lower resolution, we indeed identify Ge in the form of nanoclusters in the oxide (Fig. 7).

Thus, summarizing our results, we neither can confirm the presence of a high concentration of intermediate oxidation states at the interface nor large amounts of interfacial Ge, which have been suggested as possible culprits for poor electrical performance in the past. On the contrary, our results seem to indicate that the produced interface is quite favorable for electronics applications. This leaves the observed Ge nanoparticles in the oxide as a probable cause for worsened device properties. Nevertheless, since the oxide with the Ge nanoparticles can be etched and re-grown by deposition techniques, the atomically sharp Ge/SiO_2 interface can potentially offer a route to produce improved electronic devices.

Conclusions

In summary, we have found by a combination of experiment and simulation that oxidation of Ge-implanted Si can lead to an atomically sharp interface between Ge and SiO_2. Our ab-initio calculations and EELS measurements show that such an interface has "ideal" electrical properties with an abrupt change from the substrate to the oxide band structure, possibly enabling the use of considerably thinner gate oxides than used in current MOS devices.

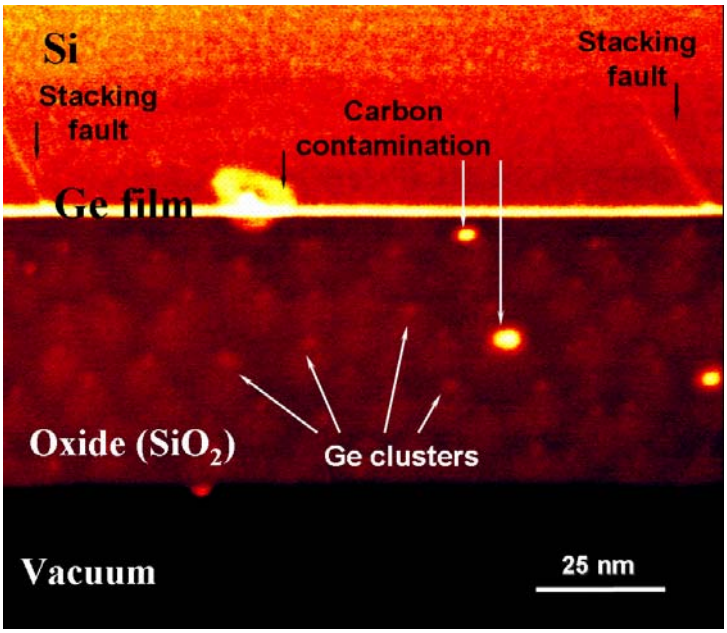

Figure 7. TEM image of the interface region with Ge nanoclusters in the oxide.

We have also proposed a Monte-Carlo model to simulate the oxidation of SiGe alloys, which explains the formation of the sharp interface due to the repulsive interaction between O and Ge, where Ge is expelled from the oxide and O atoms do not enter the Ge region under the oxidation front. For large enough pile-ups of Ge before the oxidation front, our model predicts the presence of Ge in the oxide, in agreement with experiment.

While the model predicts the general features of the process qualitatively right, it is currently not yet quantitative. The major obstacle is the lack of knowledge of the Ge hopping rates in the oxide and in Si under the oxide, where oxidation-influenced diffusion effects and interactions with the interface become important. Further work is currently ongoing to calculate the missing hopping rates from first principles.

Acknowledgments

This work was funded by the Semiconductor Research Corporation under contract number 2002-MJ-1018, the National Science Foundation under contract number 0244724, and the U.S. Department of Energy under contract number DE-AC05-00OR22725. We also thank the Ohio Supercomputer Center for supercomputer time under project number PAS0072.

References

1. D. C. Ahlgren and J. Dunn, *IBM MicroNews*, **6**, 1 (2000).
2. D. Fathy, O. W. Holland, and C. W. White, *Appl. Phys. Lett.*, **51**, 1337 (1987).
3. F. K. LeGoues, R. Rosenberrg, T. Nguyen, *et al.*, *J. Appl. Phys.*, **91**, 1724 (1989).
4. A. Terrasi, M. Re, E. Rimini, F. Iacona, V. Raineri, F. La Via, S. Colonna, and S. Mobilio, *J. Appl. Phys.*, **91**, 6754 (2002).
5. S. Iwata and A. Ishizaka, *J. Appl. Phys.*, **79**, 6653 (1996).
6. S. Lopatin, G. Duscher, T. Liang and W. Windl (to be published).

7. S. J. Pennycook and D. E. Jesson, *Ultramicrosopy*, **37**, 14 (1991).
8. G. Duscher, R. Buczko, S. J. Pennycook, *et al.*, *Ultramicroscopy*, **86**, 355 (2001).
9. N. Bonnet, N. Brun, and C. Colliex, *Ultramicroscopy*, **77**, 97 (1999).
10. J. H. Oh, H. W. Yeom, Y. Hagimoto, *et al.*, *Phys. Rev. B*, **63**, 205310 (2001).
11. T. Liang, W. Windl, S. Lopatin, *et al.*, in *2003 International Conference on Simulation of Semiconductor Processes and Devices, Cambridge, MA*, p. 143, IEEE, Piscataway, NJ (2003).
12. P. E. Batson, *J. Microsc.-Oxford*, **180**, 204 (1995).
13. A. Terrasi, S. Scalese, R. Adorno, *et al.*, *Mat. Sci. Eng. B*, **89**, 269 (2002).
14. S. J. Kilpatrick, R. Jaccodine, and P. E. Thompson, *J. Appl. Phys.*, **93**, 4896 (2003).
15. P.-E. Hellberg, S.-L. Zhang, F. M. d'Heurle, *et al.*, *J. Appl. Phys.*, **82**, 5779 (1997).
16. K. H. Heinig, B. Schmidt, A. Markwitz, et al., Nucl. Inst. Meth. Phys. Res. Sec. B **148**, 969 (1999).
17. W. Windl, T. Liang, S. Lopatin, and G. Duscher, *J. Comput. Theor. Nanosci.*, **1**, 288 (2004).
18. N. Metropolis, A. Rosenbluth, M. Rosenbluth, *et al.*, *J. Chem. Phys.*, **21**, 1087 (1953).
19. P.-E. Hellberg, S.-L. Zhang, F. M. d'Heurle, *et al.*, *J. Appl. Phys.*, **82**, 5773 (1997).
20. G. L. McVay and A. R. DuCharme, *Phys. Rev. B*, **9**, 627 (1974).
21. N. R. Zangenberg, J. Lundsgaard Hansen, J. Fage-Pedersen, *et al.*, *Phys. Rev. Lett.*, **87**, 125901 (2001).
22. J. G. Zhu, C. W. White, J. D. Budai, *et al.*, *J. Appl. Phys.*, **78**, 4386 (1995).
23. W. Windl, M. M. Bunea, R. Stumpf, *et al.*, *Phys. Rev. Lett.*, **83**, 4345 (1999).
24. K. M. Beardmore and N. Gronbech-Jensen, *Phys. Rev. E*, **57**, 7278 (1998).
25. P. Fahey, S. S. Iyer, and G. J. Scilla, *Appl. Phys. Lett.*, **54**, 843 (1989).
26. J. D. Plummer, M. D. Deal, and P. B. Griffin, *Silicon VLSI Technology*, Prentice Hall, Upper Saddle River, NJ (2000).
27. R. Buczko, S. J. Pennycook, and S. T. Pantelides, *Phys. Rev. Lett.* **84**, 943 (2000).